RHIC-II EoS Working Group White paper Contribution

S.A. Bass, H. Caines and J. Velkovska

July 12, 2006

1 Introduction

This document summarizes the activities of the Equation of State (EoS) working group within the RHIC II science initiative. The physics topics discussed in the EoS working group concentrated on the bulk properties of hot and dense QCD matter. The goal was to review the status of the field after 5 years of RHIC running and to identify the machine, detector and theoretical developments that are needed for further advance.

The key physics questions addressed are the following:

- Nature of the transition between hadron gas (HG) and Quark-Gluon-Plasma (QGP) and exploration of the QCD phase diagram.
- Thermodynamics properties of the hot and dense matter: equation of state, character of the medium, and dissipative effects.
- Thermalization mechanisms in heavy-ion collisions at RHIC.
- Hadronization mechanism.

2 RHIC II and the Detector Upgrade Programs

RHIC II is a proposed luminosity upgrade for the current RHIC accelerator. This upgrade will allow us to study processes at RHIC with very low cross-sections, and thus not accessible

at the currently available collision rates. In this section we briefly describe the predicted capabilities of the RHIC II upgrade and also the proposed detector upgrades to STAR and PHENIX. As of RHIC Run6, PHOBOS and BRAHMS have already completed their science goals and are being decommissioned.

2.1 RHIC II

RHIC II will provide a factor of 10 luminosity upgrade compared to that provided by the present accelerator (the upgrade will actually be a factor 40 increase over the initial RHIC design). Presently RHIC is limited in luminosity due to intra-beam scattering. It is planned to overcome the beam growth associated with this scattering via beam cooling with a high intensity cold electron beam. This electron cooling increases the beam luminosity by:

- Allowing the beam size to be decreased, thus increase the peak luminosity.
- Maintaining the peak luminosity over virtually the whole store.

Light-ions and protons can also be cooled in this manner, however, the improvement in luminosity drops, see Table 1. Therefore the most dramatic effects will be observed for heavy-ion beams. Neither the timing between bunches nor the space at the interaction regions are affected by the upgrade.

Au+Au 100+100 GeV/n	w.o. e-Cooling	with e-Cooling
Peak Luminosity ($10^{26} cm^{-2} s^{-1}$)	32	90
Ave. Luminosity ($10^{26} cm^{-2} s^{-1}$)	8	70
p+p 250+250 GeV		
Luminosity ($10^{32} cm^{-2} s^{-1}$)	2.4	8.0

Table 1: A comparison of beam properties at RHIC and RHIC II. Data from the RHIC accelerator division [1].

While not actually a part of the RHIC II upgrade an additional improvement planned for installation/operation in ∼2009 is an Electron Beam Ion Source (EBIS). This linac-based pre-injector is more efficient than the existing ion source, and can produce beams of all ion species, including U and polarized ^{3}He, which are not possible with the current setup.

RHIC II will maintain the ability to collide beams from injection to top energies (100 GeV/n for ions and 250 GeV for protons) as well as asymmetric systems. However, to maintain stability in the ring the asymmetric beams need to orbit with approximately equal γs.

2.2 STAR upgrades

The collaboration has several detector upgrades planned to ensure the STAR detector can take full advantage of the RHIC II era. The upgrades relevant to the EoS group are briefly described below.

2.2.1 TPC front-end electronics and data acquisition

The data acquisition (DAQ) system is being redesigned with the goal of taking data at 1 kHz. This is a significant improvement on the 50-100 Hz currently available. This rate increase will be achieved by replacing the TPC's current front-end electronics and upgrading the DAQ itself. All STAR subsystems will have such high speed DAQ capabilities by the time of the RHIC II era. The data volume resulting from such a rate will be huge and could possibly exceed our ability to store and/or analyze the information. Therefore triggers that select only the desired rare events will need to be constructed. However, this increased trigger rate, along with the RHIC II luminosity increase, will also allow us to record low energy and/or light ion minimum-bias data in significantly shorter periods of time than currently possible.

2.2.2 Time-of-Flight detector

The Time-of-Flight detector (TOF) uses Multi-Resistive Plate Chamber (MRPC) technology developed by the CERN ALICE group. A prototype of the TOF is already installed and has been used to demonstrate the clean PID abilities of the detector in the true RHIC environment. The average intrinsic timing resolution of these test MRPC modules is < 100 ps. Despite the very limited acceptance of this patch (it is only instrumented for $\pi/30$ in azimuth and $-0.5 < \eta < 0$), there are already results [2]. The full installation of the TOF is planned for fiscal year 2008, it will replace the current Central Trigger Barrel. The detector will cover the full azimuth and $-0.9 < \eta < 0.9$. Its completion will double the particle identification reach of STAR to 95% of all charged particles within the TOF acceptance. By combining the TOF measurements and dE/dx from the TPC, including that in the relativistic

rise region, full azimuthal hadron particle identification will be possible from $0.1 < p_T < 10$ GeV/c.

2.2.3 Tracking upgrades

The current design for the STAR inner vertex tracking detector consists of two tracking layers composed of monolithic CMOS pixel detectors with 30 μm square pixels. It is chiefly designed to allow the efficient topological reconstruction of open charm decays. As such the so-called Heavy Flavor Tracker (HFT), is designed to have a "point-back" resolution to the primary vertex of 50 μm or better. The layers of the HFT will be positioned at average radii of 1.5 cm and 5 cm surrounding the interaction vertex. It has $\sim$ 100 Million pixels and extends to z = $\pm$ 10 cm,(i.e. $-1 < \eta < 1$). The silicon chips will be thinned to 50 μm and mounted on a low mass carbon fiber structure. This minimizes the multiple coulomb scattering generated by the device allowing the identification of secondary vertices that are displaced by only a few 10's of microns from the primary vertex. To further reduce the material between the primary vertex and the tracking detectors the beam pipe will be replaced by one which is thin and has a smaller radius (14 mm radius, 0.5 mm thick).

In the RHIC II era the current three layers of silicon drift detector (SVT), at radii of $\sim$5, 10, and 15 cm, will need to be replaced as their readout is slow and thus incompatible with the DAQ upgrade. It is therefore proposed to replace the SVT several new layers of double sided silicon strip detectors. These will augment the one layer already installed at a radius of 25 cm, and will predominantly act as a tracking interface between the HFT and the TPC. However, the combination of inner silicon devices and the HFT could be used to improve the range of STAR's low p_T capabilities.

In addition to the direct measurement of open charm hadrons the HFT plus TOF can be used to discriminate primordial electrons from background electrons. The low mass of the HFT reduces the number of photon conversions allowing the intermediate mass dileptons range to become accessible. The HFT plus TOF combination can therefore be used to identify short-lived vector mesons, such as the ϕ and ω, via their electromagnetic decays. It is estimated that this combination of detectors will increase STAR's sensitivity to electromagnetic vector meson decays by a factor of 20-40.

Tracking upgrades are also envisioned in the forward rapidity region using silicon disks and a triple GEM technology based chamber. The exact designs for these detectors are still being

completed but it is planned to provide precision tracking in the $1 < \eta < 2$ range.

2.3 PHENIX upgrades

The PHENIX detector was designed to detect rare events in heavy ion and p+p collisions. It combines a large bandwidth DAQ and trigger system with a highly granular detector optimized to measure photons, electrons/positrons, muons and high p_T hadrons. The goal of the PHENIX upgrade program is to provide the tools necessary to obtain key measurements that are presently beyond the capabilities of the PHENIX detector and combined with the upgraded luminosity will not only enable PHENIX to remain competitive well beyond the turn-on of LHC but will also advance our understanding of QCD by addressing the following subjects:

- The study of QCD matter at high temperatures with heavy ion, p-nucleus, and p+p collisions. These studies include high p_T phenomena using identified hadrons in the p_T range 3 – 10 GeV/c and $\gamma-$jet correlations, thermal radiation and effects of chiral symmetry restoration in the electron-pair continuum, in particular at low masses ($< 1\text{GeV}/c^2$), production of mesons with open charm and beauty and quarkonia spectroscopy including excited states.
- Extended exploration of the spin structure of the nucleon by measurements of the gluon spin structure (using heavy flavor and γ-jet correlations), quark spin structure (via W-production) and transversity.
- Exploration of the nucleon structure in nuclei.

The PHENIX upgrades that are relevant to the physics of the QCD EoS are briefly summarized below. The program provides for high momentum particle identification, accurate vertex tracking, and forward capabilities.

2.3.1 Si Vertex tracking

The vertex tracking is based on highly segmented silicon strip or pixel detectors at mid rapidity and silicon pixel detectors in the forward rapidity region. The central detectors (silicon barrel) cover pseudo-rapidity $-1.2 < \eta < 1.2$ and almost 2π in azimuth and provide

a single-track resolution of 50 μm at the vertex. The forward silicon detectors are designed to provide coverage in the angular acceptance of the forward muon arms. The acceptance covers $1.2 < |\eta| < 2.7$ and the almost full azimuth angle with a resolution of 150 μm.

With the present PHENIX detector, heavy-quark production has been measured indirectly through the observation of single electrons. These measurements are inherently limited in accuracy by systematic uncertainties resulting from the large electron background from Dalitz decays and photon conversions. In particular, the statistical nature of the analysis does not allow for a model-independent separation of the charm and beauty contributions. The tracking provided by the VTX detector will allow for suppressing the background in the electron measurements by several orders of magnitude and thereby obtaining a clean measurement of of heavy flavor production in the single electron channel. Additionally, because the lifetime of mesons with beauty is significantly larger than that of mesons with charm, the VTX information will allow to disentangle charm from beauty production over a broad p_T range. In the hadron channel, the vertex cuts will reduce the combinatorial background of K and π to an extent that a direct measurement of D mesons through this decay channel will become possible. In addition, the VTX detector will substantially extend the p_T coverage for charged particles and combine with the high-p_T PID detector will allow for flavor-tagged jet measurements and correlations.

2.3.2 PHENIX Nose Cone Calorimeter (NCC)

The PHENIX Nose Cone Calorimeter will instrument the pole pieces of the PHENIX axial field magnet with a compact, dense sampling calorimeter using tungsten plates interleaved with silicon readout. These will provide forward photon and jet coverage for the PHENIX heavy ion and spin measurements. Coupled with the forward Si-VTX tracker, the NCC will allow for π^0 identification and flow measurements in the forward rapidity region ($0.9 < |\eta| < 3.0$).

2.3.3 PHENIX high-p_T detector

The baseline PHENIX detector is equipped with a scintillator based TOF wall which covers $\Delta\phi = 45^o$ in the central rapidity region $-0.35 < \eta < 0.35$ in the PHENIX East arm. The timing resolution of $\sigma \approx 100$ ps allows for π/K and K/p separation up to $p_T = 2.5$ and 4.5 GeV/c, respectively. Measurements using this device have lead to the discovery of the

enhanced baryon production at intermediate $2 < p_T < 4$ GeV/c in central $Au + Au$ collisions. In this range, the hadron production was shown to be sensitive to the hadronization mechanism in the hot and dense medium (see discussion in section 6). Hadron identification out to high-p_T is needed for the detailed study of the hadronization and, in particular the interplay between recombination and fragmentation of quarks. The PHENIX detector is upgraded with a high-p_T detector which includes and Aerogel Čerenkov detector and a TOF detector based on MRPC technology. The Aerogel detector has already been installed in the PHENIX West arm for Run4, while the TOF detector will become fully operational in Run7. This system will allow for track-by-track identification of π, K, p out to $p_T \approx 9$ GeV/c. The coverage is limited: $-0.35 < \eta < 0.35$ and $\Delta\phi = 22^o$, but nevertheless it will make possible the measurements of identified particle yields, ratios, correlations and flow in the transverse momentum range which is important for the study of the hadronization mechanism.

3 Exploration of the QCD EoS and the Phase Diagram of Nuclear Matter in a Fundamental Theory

3.1 Lattice QCD equation of state

Lattice gauge simulations of QCD [3, 4] (LQCD), provide a unique opportunity to study the *equation of state* (EoS) and the phase diagram of strongly interacting QCD matter within a fundamental theory. In principle, both the non-perturbative hadronic matter and the non-perturbative QGP phases of QCD can be investigated. The lattice results show that non-perturbative effects dominate the EoS in the temperature regime attainable by the experiments at RHIC. Strong deviations from ideal gas are observed for temperatures $T < 2\ T_c$ [5, 6] and have been attributed to remnants of confinement. At temperatures $T \sim 2 - 4\ T_c$ the lattice results remain about $15 \pm 5\%$ below the ideal gas limit indicating that non-perturbative effects are important even at high temperatures.

Within the first few years of experimental exploration the RHIC experiments have gathered evidence that the intuitive picture of the high temperature phase as a gas of weakly interacting quarks and gluons, which is based on leading order perturbation theory, is incorrect. The matter produced at RHIC can be characterized as a strongly interacting medium whose energy density and temperature clearly exceed the critical values predicted from LQCD for the transition from ordinary hadronic states to a strongly interacting Quark-Gluon Plasma

(sQGP) [7]. The deviations from the ideal gas EoS observed on the lattice and the implications of the existence of bound states above T_c have still to be explored and connected to the experimental observables through dynamical models, as discussed in Section 4. Other LQCD results that can be tested experimentally are the nature of the transition between hadron gas and QGP and the existence and location of a critical point in the QCD phase diagram.

3.2 The LQCD phase diagram and the search for the critical point

LQCD provides a non-perturbative approach to the description of the physical mechanisms at the origin of color confinement and chiral symmetry restoration. This is done via the computation of thermodynamic averages of different quantities related to hadron masses and widths, as well as quantities related to the bulk properties of the medium and the phase transition. A question of great importance in that context is that of the order of the deconfinement phase transition or if it is a smooth cross-over. This is crucial information since many striking QGP signatures depend heavily on the assumption of a first order phase transition and the existence of a (long-lived) mixed phase of QCD matter.

Calculations at vanishing baryon chemical potential suggest that for physical values of the quark masses (two light (u, d)-quarks and a heavier $s-$quark) the deconfinement transition is a rapid cross-over rather than a first order phase transition with singularities in the bulk thermodynamic observables [8]. The critical temperature at $\mu_B = 0$ for the rapid cross over in the (2+1) flavor case was recently predicted to be $T_c = 172 \pm 11$ MeV [9].

However, many QCD motivated calculations for low temperatures and high baryon densities exhibit a strong first order phase transition (with a phase coexistence region) [10, 11]. These two limiting cases suggest that there exists a critical point (second order phase transition) [12] at the end point of a line of first order phase transitions. Recently, the exploration of the phase diagram for large temperatures and small, but non-vanishing, values of the baryon chemical potential became possible through the application of novel techniques, such as Ferrenberg-Swendsen re-weighting [13], Taylor series expansions [14, 15] or simulations with an imaginary chemical potential [16, 17]. Although these techniques have allowed for considerable improvements, the location of the critical point in the $T - \mu_B$ plane still has large theoretical uncertainties, due to the sensitivity to the quark masses and the lattice sizes used in the calculations. The predicted value of $\mu_B^{endpoint}/T_c$ varies between $\mu_B^{endpoint}/T_c \simeq 1 - 3$ [19, 20, 21], i.e. $\mu_B^{endpoint}$ =170 – 420 MeV, assuming T_c stays constant at $T_c =$

170 MeV. Lacking better theoretical guidance, the discovery of the critical point can only be possible by a systematic experimental exploration of the QCD phase diagram. The proposed signatures are commonly based on the fact that at the critical point is a genuine thermodynamic singularity at which the quark number susceptibilities diverge and the order parameter fluctuates on long wavelengths. The simplest proposed observables are the event-by-event fluctuations of the mean transverse momentum $\langle p_T \rangle$ of the charged particles in an event, and of the total charged multiplicity in an event [23]. One expects that as the control parameter is varied, the signatures would strengthen and then weaken again as the critical point is approached and then passed. The baryon chemical potential can be varied experimentally by dialing of the center of mass energy, $\sqrt{s_{NN}}$, of the collisions. This could thus serve as the control parameter in the search for the critical point in the QCD phase diagram.

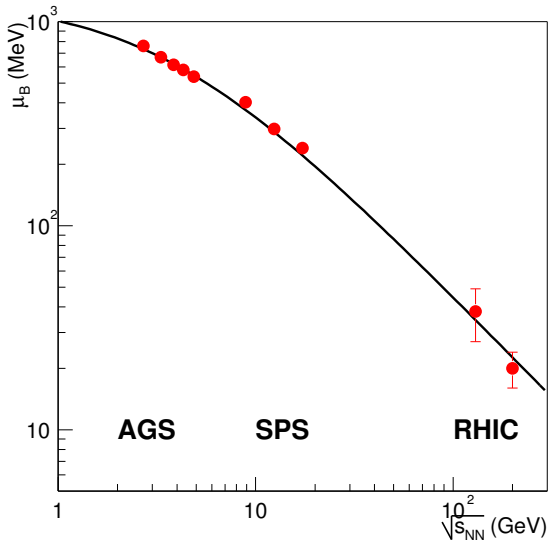

Figure 1: μ_b vs $\sqrt{s_{NN}}$ from statistical model fits to mid-rapidity data from the AGS, SPS, and RHIC. The fit data and the parametrization are taken from [34].

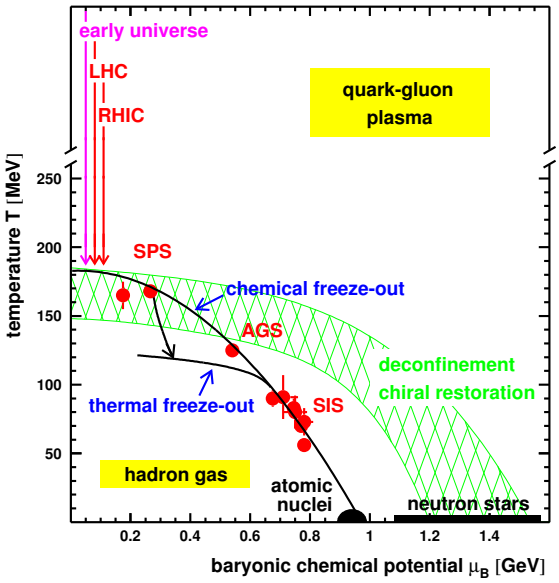

Figure 2: μ_b vs T_{ch} calculated from statistical model fits to mid-rapidity data from the AGS, SPS, and RHIC. The figure is taken from [35].

Considerable amount of experimental data spanning $\sqrt{s_{NN}} = 2.7 - 200$ GeV already exists from measurements at the AGS, SPS and RHIC. Analysis of particle abundances using statistical thermal models allows for the determination of the baryon chemical potential and the temperature at chemical freeze-out (T_{ch}), assuming the system is in thermal equilibrium. It has been noted that for $\sqrt{s_{NN}} \geq 8.9$ GeV (SPS fixed target energy of 40 AGeV) and

above, the calculated T_{ch} reaches the critical temperature predicted by LQCD. This possibly implies that the hadron yields are frozen in at the phase boundary. However, the order of the transition and the evolution with μ_B are still open questions. Various experimental studies searching for event-by-event fluctuations in apparent temperature, mean transverse momentum [24, 25, 26, 27, 28], multiplicity [29], net charge [30, 31, 32], and momentum correlations [33] have been performed. In all cases, the excitation functions show little or no change between the SPS and RHIC energy and no indication of exceedingly large signals as expected in the vicinity of the critical point. Following the parameterization of μ_B at mid-rapidity as a function of $\sqrt{s_{NN}}$ [34], we estimate that the range of $\mu_B = 70 - 240$ MeV remains unexplored (see Fig. 1). An energy scan between 20 GeV $< \sqrt{s_{NN}} <$ 62 GeV should complete the exploration of the phase diagram at mid-rapidity and possibly locate the critical point. At least three data sets (steps of 50 MeV in μ_B) with statistics comparable to the RHIC Run4 are needed to allow for detailed correlation and fluctuation measurements at each $\sqrt{s_{NN}}$. An energy scan including even lower energies (5 GeV $< \sqrt{s_{NN}} <$ 62 GeV) which smoothly overlap the regions of the AGS and SPS data and fill the gap between SPS and RHIC are also under consideration. The technical challenge for running RHIC at such low energies comes from the requirement to operate the RHIC magnets at very low currents, which in turn translates into instabilities in the magnetic field. Initial machine studies aiming to overcome these limitations have already begun and have shown promising results [36]. If successful, RHIC will be the only facility in the world that can provide a comprehensive data set spanning 5 GeV $< \sqrt{s_{NN}} <$ 200 GeV ($\mu_B = 30 - 536$ MeV) and thus aim for a systematic search for the critical point. Obtaining the data at the same facility with the same detectors also provides a superb control of the experimental systematic errors. In order to be completed in a reasonable time, these studies require RHIC II luminosities.

If the critical point is located at higher baryon chemical potential ($\mu_B \geq 500$ MeV) , it may be accessible at the future GSI facility. However, statistical model calculations using SPS, AGS, and SIS data, represented in Figure 2 [35], indicate that at the collision energies required to produce such high baryo-chemical potentials it is questionable if the QGP phase is reached. At RHIC a system with initial temperature higher than T_c and baryon density comparable to low energy SPS can be created at forward rapidities. Thermal model analysis of the particle ratios measured by the BRAHMS experiment [37] show that at $y = 3$, μ_B is about 100 MeV larger than at mid-rapidity. Thus, measurements away from the central rapidity region will expand the experimentally accessible region of the phase diagram. Fluctuation and correlation measurements at forward rapidities will be possible after the PHENIX Nose-Cone Calorimeter (NCC) and forward Si-tracker upgrades and the STAR forward meson

spectrometer and forward tracker upgrades. However, the full particle identification (PID) capabilities that are necessary for the characterization of the chemical properties of the system will be lost, since the BRAHMS experiment is phased out and comparable PID coverage is currently not provided for in the planned future PHENIX and STAR upgrades.

4 Dynamical evolution of the QCD medium

4.1 Theoretical tools and comparison to data

The main disadvantage of lattice simulations is the practical restriction to finite, periodic systems in global equilibrium, a scenario far removed from the highly inhomogeneous off-equilibrium situation found in complex heavy-ion reactions.

In order to connect the theoretical thermodynamic properties of a QGP with experimental data on finite nuclear collisions, the dynamical effects of the collisional environment need to be estimated. Transport theory is the basic tool to address this task. Non-equilibrium effects are certain to arise from the rapid time-dependence of the system (even the use of the term "state" seems questionable), finite size effects, inhomogeneity, N-body phase space, particle/resonance production, and freeze-out and collective dynamics. Microscopic and macroscopic (hydrodynamical) transport models attempt to describe the full time-evolution from an assumed initial state of the heavy ion reaction (i.e. the two colliding nuclei or a thermalized QGP) up to the freeze-out of all initial and produced particles after the reaction.

Hydrodynamical models neglect most of the non-equilibrium effects by making the assumption that the initial condition can be assumed to be in local thermal equilibrium and that local equilibrium is maintained during evolution. Even more simple *fireball* or *blast-wave* models simply parameterize final spectra and abundances via freeze-out parameters, e.g. $T, \mu_B, \vec{v}_f$.

Nevertheless, Relativistic Fluid Dynamics (RFD, see e.g. [38, 39, 40]) is ideally suited for the *QGP and hydrodynamic expansion* phase, but breaks down in the later, dilute, stages of the reaction when the mean free paths of the hadrons become large. The biggest advantage of RFD is that it directly incorporates an equation of state as input and thus is so far the only dynamical model in which a phase transition can explicitly be incorporated. In the ideal fluid approximation (i.e. neglecting off-equilibrium effects), the EoS is the *only* input to

the equations of motion and relates directly to properties of the matter under consideration. The observables that are sensitive to the dynamical evolution of the system are the identified single particle spectra and elliptic flow. A wealth of experimental data on identified particle spectra and flow measured as a function of centrality, transverse momentum, beam energy and colliding species already exist from Run1 - Run5 at RHIC. The hydrodynamics description has been very successful [41, 42, 43] in describing the collective behavior of the system. In particular, RFD has been able to reproduce the characteristic mass dependence in the p_T dependence of elliptic flow at low-p_T ($p_T < 1.5$ GeV/c). The mass scaling is sensitive to the EoS used in the calculations. It has been shown that the agreement with the data requires a QGP EoS [44, 45]. However, these calculations use an EoS with a strong first order phase transition and ideal parton gas to describe the plasma phase which is inconsistent with the lattice results. It has been noted that the details of phase transition do not lead to significant dynamical effects [41] as long as the total increase of the entropy density across the transition, as observed in the lattice data is well reproduced by the model. If this is the case, then the experimental sensitivity to the details of the EoS evolution may be questioned. On the other hand the v_2 experimental results can clearly discriminate between hydrodynamics calculations with latent heat varying between $\delta\epsilon_{lat} = 0.4, 0.8, 1.6$ GeV/fm^3, which indicates that the strength of the phase transition is important for agreement with the data. The latent heat and the order of the phase transition also influence the space-time dynamics observable through the HBT radii of the particle emission source. Viscous corrections were shown to improve the agreement with the data [46], but there are also indications that a cross-over phase transition or non-Bjorken initial conditions may help to resolve the "HBT-puzzle" [47, 48].

Attempts to incorporate a parameterized lattice results into hydrodynamics calculations have just begun [49, 50, 51]. Such studies are crucial for establishing the evolution of the EoS in relativistic heavy ion collisions. However, a complete and consistent account for all experimental data can not be achieved without a proper description of the properties of the medium (e.g. viscosity) at all stages of the collisions and relaxing the assumption of boost invariance.

Presently, most hydrodynamics calculations are 2+1 dimensional and thus limited to a slice around mid-rapidity [41, 42]. The shape of the spectra as well as the transverse momentum dependence of the elliptic flow for minimum bias data are reproduced nicely, but more specific centrality bins pose a problem for the elliptic flow calculations. In order to reproduce simultaneously the shape of the particle spectra (which freeze-out at $T_{kinetic} = 110$ MeV) and

the measured hadron abundances (determined at the chemical freeze-out $T_{ch} = 170$ MeV) , the ideal hydrodynamics calculations implement into the EoS temperature dependent individual non-equilibrium chemical potentials. Alternatively, the ideal hydrodynamics has to be coupled with a "hadronic afterburner" (see discussion in section 5.1).

Recently, fully three-dimensional calculations have become available as well [43, 88] and a first successful comparisons to spectra, multiplicity distributions and elliptic flow data [52] measured at forward rapidities have been made.

Exploring the choice of initial conditions, implementing a lattice-base EoS and viscosity throughout the system evolution within a 3D hydrodynamics model coupled with hadronic cascade remains a theoretical challenge for future and should be made one of the top priorities of the RHIC theory effort. In the next section we concentrate on measurements that will provide additional experimental constraints to the theory and require the RHIC II capabilities.

4.2 Experimental approaches to the QCD EoS in the RHIC II phase

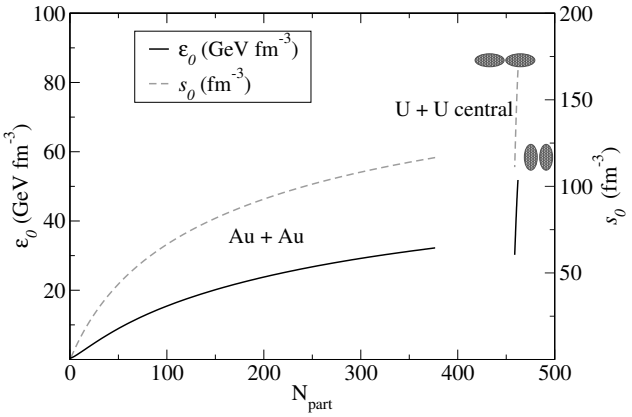

Figure 3: Peak energy density (left axis) and entropy density (right axis) vs the number of participants for various Au+Au impact parameters and U+U full-overlap collisions both at $\sqrt{s_{NN}} = 200$ GeV. Figure taken from [53].

Full-overlap U+U collisions provide significantly larger initial energy densities at comparable spatial deformation, and significantly larger deformation and volume at comparable energy

density, than semi-central Au+Au collisions. It has been shown quantitatively that this provides a long lever arm for studying the hydrodynamic behavior of elliptic flow in much larger and denser collision systems and the predicted non-linear path-length dependence of radiative parton energy loss [53, 54]. This is of particular importance for the study of the QCD equation of state since systematic studies of the elliptic flow at mid-rapidity in Au+Au and Pb+Pb collisions of varying centrality at the AGS, SPS, and RHIC [56, 57] show that the ratio of the elliptic flow coefficient over the spatial eccentricity, v_2/ϵ_x, scales with the charged multiplicity density per unit transverse area, $\frac{1}{S}\frac{dN_{\rm ch}}{dy}$. Which is in turn proportional to the initial entropy density s_0 of the reaction zone. A similar scaling is seen when studying v_2/ϵ_x as a function of rapidity in minimum bias Au+Au collisions at RHIC [58, 59, 60]. Predictions from ideal fluid dynamics [61] agree with the data only at the top RHIC energy, in almost central Au+Au collisions, and at mid-rapidity, i.e. where the highest initial entropy densities are created. As one moves to more peripheral collisions, lower collision energies, or away from mid-rapidity, the measured elliptic flow begins to increasingly fall below the ideal fluid limit. According to Figure 25 in [57], the data do not seem to approach the ideal fluid limit gradually, but follow a trend which seems to *cross* the hydrodynamic curve near $\frac{1}{S}\frac{dN_{\rm ch}}{dy} \approx 25/\mathrm{fm}^2$ [62]. This is unexpected since the ideal fluid value for v_2/ϵ_x is an upper limit which should not be exceeded [63]. It is therefore very important to check that at larger values of $\frac{1}{S}\frac{dN_{\rm ch}}{dy}$ the data indeed settle down to the hydrodynamic prediction. If they do not, this would imply a stiffer QGP equation of state than so far assumed since the hydrodynamic value of v_2/ϵ_x increases with the speed of sound [64]. With Au+Au collisions the only possibility to further raise $\frac{1}{S}\frac{dN_{\rm ch}}{dy}$ is to increase the collision energy, which will be possible at the Large Hadron Collider (LHC). It has however been shown that with full-overlap U+U collisions at top RHIC energies in edge-on-edge geometry, one can increase $\frac{1}{S}\frac{dN_{\rm ch}}{dy} \sim s_0$ by $\approx$55%, to values around 40 fm^2 [53, 54], Figure 3. This is a larger gain than between Au+Au collisions at impact parameters $b = 0$ and $b \simeq 10$ fm. On the experimental side, the use of uranium beams requires the Electron Beam Ion Source, which is planned to begin operation in 2009 [55], thus the proposed measurements could be available from RHIC on the same timescale as the first data from the LHC.

Direct photons provide another venue for studying the QGP equation of state: These can be categorized into high transverse momentum *prompt* photons originating from hard pQCD processes during the initial stage of the reaction and *thermal* photons radiated during the evolution of the thermalized QGP and hadron gas phases of the medium. The most prominent processes for the creation of direct photons in a QGP are $q\bar{q} \rightarrow \gamma g$ (annihilation) and $gq \rightarrow \gamma q$ (Compton scattering) [65]. The production rate and the momentum distribution

of the photons depend on the momentum distributions of quarks, anti-quarks and gluons in the plasma and have been shown to depend on the QGP equation of state [66, 67, 68, 70].

Among the most clear evidences for QGP formation from QCD calculations on the lattice are: (i) the sharp rise of $g \propto \varepsilon(T)/T^4$, or equivalently $g \propto s(T)/T^3$, at temperatures around T_c, and (ii) the flattening of the same EoS curve above T_c. The sharp jump is, of course, due to the sudden release of a large number of (partonic) degrees of freedom at T_c. The subsequent plateau is due to the full formation of a QGP with a *fixed* (constant) number of degrees of freedom for increasingly higher temperatures. It has been proposed in [71] to use the inverse slope parameter of the thermal photon spectrum, T_{eff}, as a proxy of the temperature of the produced hot medium, and study the quantity $(dN_{ch}/d\eta)/T_{eff}^3$ as a function of centrality in order to obtain information on the shape of $g(T) \propto s_0/T_0^3$. One has to note that though transverse flow effects do influence the direct proportionality between the slope and the temperature of the photon spectrum [70] (specifically at low p_T and in the SPS regime), according to [71] the slope parameter and the real temperature T of the source are seemingly still correlated at RHIC energies. The approach of d'Enterria and Peressounko [71] has been tested using a 2D+1 Bjorken hydrodynamical model that reproduces well the existing hadron and photon spectra measured in Au+Au collisions at $\sqrt{s_{NN}} = 200$ GeV. These calculations demonstrate that by using the hadron and photon data in such a way, one can indeed disentangle between an underlying medium with hadron-resonance-gas (with rapidly rising number of degrees of freedom) or QGP-like (with fixed number of g above T_c) EoS. On the other hand, the model indicates that at top RHIC energies and for most of the centralities, the hottest parts of the initial fireball are in the QGP phase, and the aimed observation of a rise in g around T_c is only barely seen (if at all) for the very most peripheral reactions. Thus, direct evidence of the QGP-HRG phase change itself via the study of the centrality dependence of the hadron multiplicities and thermal photon slopes would only be potentially feasible at RHIC II in Au+Au reactions at *lower* center-of-mass energies ($\sqrt{s_{NN}} \approx$ 20 – 65 GeV). In any case, more quantitative conclusions on the possibility to extract the exact shape of the underlying EoS and/or the absolute number of degrees of freedom of the produced medium require more detailed theoretical studies (e.g. with varying lattice-inspired EoS's and/or using more numerically involved full 3D+1 hydrodynamical approaches).

An alternative way to extract the QGP equation of state sensitive thermal photon yield from the data is by means of photon HBT interferometry [72, 73, 74, 75, 76, 77, 78], where the yield information of the direct photons is encoded in the λ-factor of the three-dimensional correlation function. The advantage of the HBT analysis is that it allows to determine

the total direct photon yield independently of integrating the background-subtracted direct photon spectrum, allowing for an important cross-check regarding this quantity.

It has been suggested in [79] to use a combination of entropy- and energy-density measurements in order to determine the number of degrees of freedom of the system via $g \sim s_0^4/\epsilon_0^3$. Again, the initial entropy density can be inferred from the final particle multiplicity or from an analysis of the composition of the fireball at chemical freeze-out [80]. An independent experimental proxy of the initial energy density is not easily obtained however. Indeed, due to longitudinal work any measurement of the *final* transverse energy density, $dE_T/d\eta$, provides only a *lower limit* on the initial ϵ_0. The proposal of the authors of extracting (an upper limit of) the energy density from jet quenching data ("punch-through" measurements) is not obvious either, since parton energy loss measurements provide information on the attained *particle* density rather than on the *energy* density of the system. Although more studies are needed in order to identify experimental observables closely related to ϵ_0, which one can then use to obtain $g \sim s_0^4/\epsilon_0^3$, an energy scan between SPS and top RHIC energies ($\sqrt{s_{NN}} \approx 20$ – 65 GeV) would again be of high interest for the study of the evolution of the EoS of the underlying medium for different initial thermodynamical conditions.

5 Properties of the medium

5.1 Viscosity

The agreement of ideal hydrodynamic predictions of differential elliptic flow and radial flow patterns with Au+Au data at $\sqrt{s_{NN}} = 200$ GeV and $\sqrt{s_{NN}} = 130$ GeV has provided evidence for the nearly perfect fluid properties of the strongly coupled Quark Gluon Plasma, sQGP, produced at RHIC. "How perfect is the sQGP fluid ?" is an important question that can not be answered within a framework that does not allow for dissipative effects. Since the relativistic Navier-Stokes equation cannot be solved directly, including dissipation in the sQGP phase presents a challenge to the theory. Estimates based on numerical solutions of the Navier-Stokes equation coupled with a boost-invariant blast-wave model [81] show that the viscosity affects both the radial and elliptic flow, as well as the HBT radii. Such studies provide an upper limit to the shear viscosity in the sQGP $\Gamma_s \equiv \frac{4}{3}\frac{\eta}{\epsilon+p} \sim 0.1$ [82]. This estimate provided a surprisingly small finite lower bound for the viscosity over entropy ratio of η/s, well in tune with the success of ideal hydrodynamic calculations at RHIC.

Utilizing lattice calculations, a first attempt on determining the shear viscosity has been made in [83], however with large error-bars. It is unlikely that the viscosity can be determined reliably from lattice calculations. This is an area where experimental advances coupled with phenomenological models remains the most viable approach.

It has been recognized that the strong dissipation in the hadron gas stage and the assumptions about hadro-chemical and thermal equilibrium after the sQGP hadronizes have important implications [84]. The perfect fluidity in the sQGP has been attributed to the sudden increase of the entropy density of QCD matter at the critical temperature T_c, rather than anomalous reduction of viscosity. This type of data analysis implements a hybrid model ("hydro+micro").

Hybrid models [85, 86, 87, 88] that combine the RFD calculation with a microscopic hadronic cascade model have the key advantage that the freeze-out occurs naturally as a result of the microscopic evolution and that flavor degrees of freedom are treated explicitly through the hadronic cross-sections of the microscopic transport. The microscopic treatment of the hadronic phase automatically incorporates viscosity for that phase in the calculation. Matching the conditions between the two phases in the calculations is typically done by choosing a temperature (near T_{ch}) at which hadronization occurs. Disentangling the contributions to the elliptic and radial flow and thus deducing the viscosity of the medium requires experimental input. Measurements involving identified particles which have small hadronic cross-sections (ϕ, Ω, Ξ) provide suitable probes, since they are mostly sensitive to the sQGP phase of the collisions. Experimentally, these measurements require large amounts of data, since the particles under consideration are rarely produced. The present status of v_2 measurements for strange particles from the STAR experiment [89] are shown in Figure 4. Data including v_2 of ϕ mesons measured in minimum bias $Au + Au$ collisions in the PHENIX experiment [90] are shown in Figure 5. Although both data sets are still preliminary, they incorporate most of the available statistics from Run4 at RHIC, which is the largest data set obtained from $\sqrt{s_{NN}} = 200$ GeV $Au + Au$ collisions so far. The results present tantalizing evidence that $\Xi^- + \overline{\Xi}^+$, $\Omega^- + \overline{\Omega}^+$, and ϕ participate in elliptic flow, which is predominantly partonic. There are also indications that the strength of the flow signals depend on the number of quarks in the hadrons. However, the statistical errors in these measurements are large and prevent any detailed comparison with theory. It is desirable to study the centrality dependence of v_2 and to do this separately for particles and anti-particles, however with the present statistics this can only be done at the expense of even larger statistical error bars and less discriminating power against theoretical models. The precision study of the elliptic

flow for multi-strange particles requires the RHIC II luminosity. These measurements provide important constraints to the description of the sQGP phase of the collisions and will ultimately give a handle with which to disentangle the viscous effects in the partonic and hadronic stages.

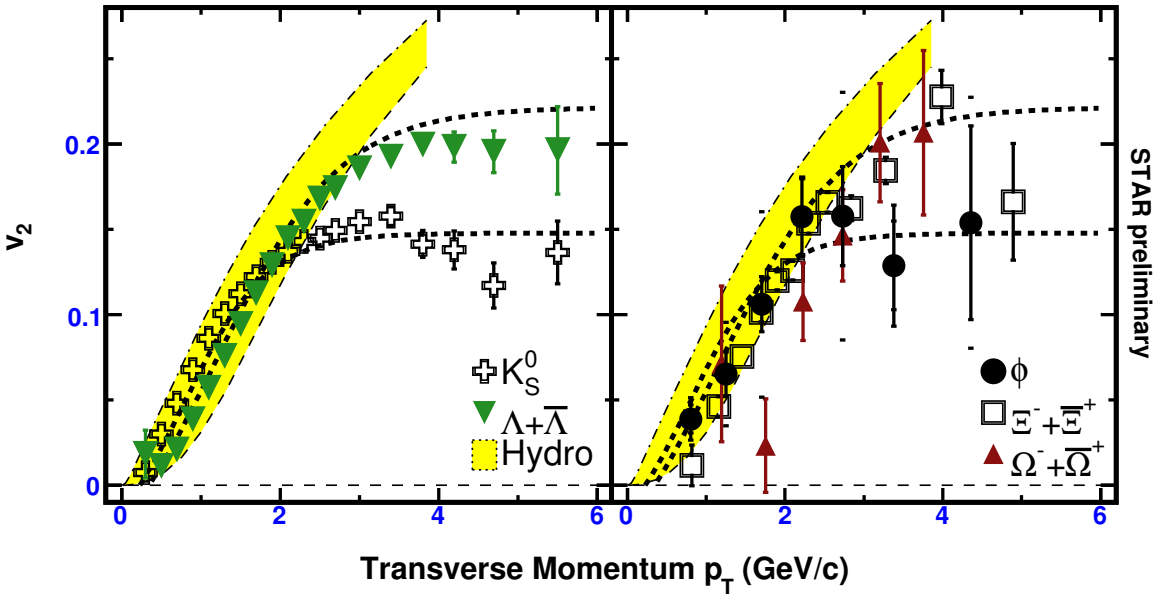

Figure 4: Azimuthal anisotropy v_2 for strange hadrons (left) and multi-strange hadrons (right) in 200 GeV minimum bias Au+Au collisions. The dashed lines show a common fit [91] to the K^0_S and $\Lambda+\overline{\Lambda}$ data. Hydrodynamic model calculations are shown as shaded areas.

It has been suggested that the simultaneous directed flow measurement of v_2 and v_3 in asymmetric collision systems would provide the most efficient way of constraining fully 3D hydrodynamic calculations and show an increased sensitivity to the viscosity of the medium. In order to provide the necessary accuracy, RHIC would need to provide statistics for A+B collisions at a level comparable to current Run 4/5 statistics. Note that this particular measurement would require the large rapidity coverages of the PHOBOS and BRAHMS experiments. Since these are currently being phased out, an equivalent capability needs to be recovered with future STAR and PHENIX upgrades.

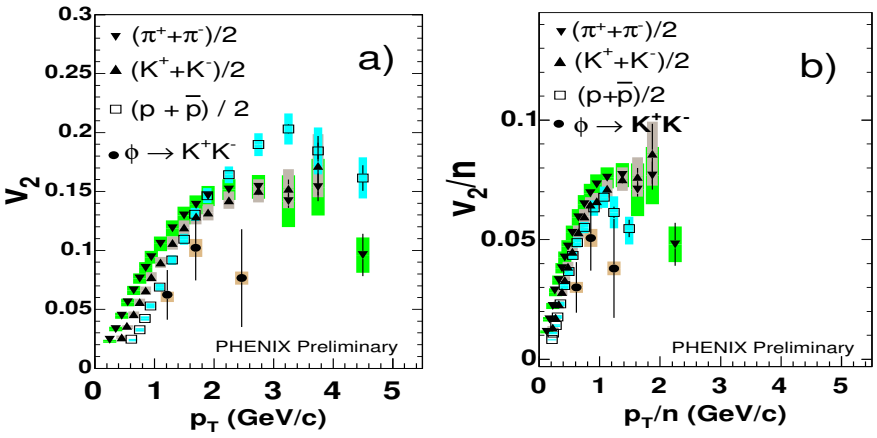

Figure 5: (a) v_2 of the ϕ mesons as a function of p_T, and (b) v_2/n of the ϕ as a function of p_T/n, (n being the number of quarks), measured in minimum bias $Au + Au$ collisions at $\sqrt{s_{NN}} = 200$ GeV by the PHENIX experiment. The bands around the data points represent the systematic errors. Results for other identified hadrons are plotted for comparison.

5.2 Transport coefficients

Theoretically, the determination of transport coefficients, such as shear viscosity, heat capacity and diffusion coefficients are among the major challenges for the near- and medium-term future. Charge diffusion and electric conductivity has been studied using LQCD in [92]. These calculations benefit from the correlator on the lattice being less noisy than for the viscosity, so progress in this area should be possible on rather short time-scales. Overall, the study of heavy-quark diffusion should be easiest on the lattice, whereas no work so far has been done on the extraction of the heat capacity, which might be the most difficult to obtain.

One of the most promising approaches for making progress in the area of transport coefficients is the sector of heavy-flavor thermalization. The charm diffusion coefficient can be related to the charm energy loss and momentum broadening. Utilizing transport theory, these quantities can then be used as an input for the calculation of charm elliptic flow, thus creating a relation between an experimentally accessible quantity and the diffusion coefficient [93, 94, 95].

Along similar lines, recent work on the possible creation of Mach-cones [96, 97, 98, 99] or Čerenkov radiation [100] in the QCD medium through the passage of high-p_t particles may reveal important information on the transport properties of the medium. Structures consis-

tent with Mach cones have been observed in the data [101, 102]. However, the theoretical interpretation of the data is still incomplete and parameter dependent [103].For example, Mach-cones were not observed when nonlinear hydrodynamic response to the jet was estimated with 2+1 dimensional hydro code [104]. Further advance will require more theoretical work as well as more detailed experimental input. RHIC II luminosity is important as the experimental observables require multi-particle correlations.

5.3 Thermalization

Establishing a thermalized system is an important pre-requisite of for a state of matter to be formed. Thus here we examine the evidence that a thermalized system has been formed in $A + A$ collisions at RHIC, the timescale for thermalization to occur, the experimental observables that may establish links to theoretical models of thermailization.

5.3.1 Evidence for thermalization

Hadron abundances measured in relativistic heavy ion collisions have been successfully described using statistical thermal models. A system in a chemical equilibrium with chemical freeze-out temperature $T_{chem} \approx 170$ MeV is observed independent of collision system and collision centrality. This temperature agrees with the value for the quark-hadron phase transition temperature predicted by Lattice QCD. The system expansion and the hadronic re-scattering may still continue after chemical equilibration. At kinetic freeze-out, when the hadrons stop interacting, the temperature is reflected in the slopes of the hadron momentum distributions. The kinetic freeze-out temperature can be extracted by comparing the measured spectral shapes of identified hadrons to a hydrodynamic model that has been tuned to reproduce the data. The model shows that it takes about 9-10 fm/c until the fireball has become sufficiently dilute to completely convert to hadronic matter, and another 7-8 fm/c to completely decouple and a temperature of $T_{kinetic} \approx 100$ MeV. The success of the statistical thermal models and the hydrodynamics description of single particle spectra and yields implies that the matter produced at RHIC has reached thermal equilibrium at some stage of its evolution.

5.3.2 Timescale for thermalization

The thermalization process due to its highly non-equilibrium nature is difficult to model theoretically. An important step in understanding the thermalization mechanism is to determine experimentally the timescale on which thermalization occurs. One way to do that is to compare a dynamical macroscopic model of the system evolution to experimental data and then infer the timescale of thermalization from the model.

Since the spectral shapes evolve throughout the system's life, they do not carry sufficient information that allows to constrain the equilibration time. The elliptic flow ($v2$), on the other hand, is driven by the spatial anisotropy of the reaction zone and the resulting anisotropic pressure gradients that feedback into the system to reduce the spacial anisotropy. This self-quenching mechanism quickly bring the system into a spherically symmetric state after which the $v2$ strength saturates. At RHIC energies this saturation happens before the completion of hadronization, and thus it can be used a s clock to estimate the time duration . The hydrodynamics approach being a macroscopic description of the system is not applicable to describe the pre-equilibrium stage of the reaction and can not give an answer on how thermal equilibrium is achieved. It can, however, give an estimate of the time it takes for the system to reach local thermal equilibrium by connecting the measured v2 and the evolution of the pressure gradients in the system. The success of ideal hydrodynamics in describing the large elliptic flow observed at RHIC requires very short thermal equilibration times, of the order $\tau_{therm} < 1\text{fm}/c$.

5.3.3 Thermalization mechanism and links to experiment

The thermalization process itself can only be assessed using a microscopic description of the pre-equilibrium system dynamics. Microscopic transport models are applicable in this case. These models need experimental input to constrain the transport coefficients in the medium. Heavy quarks are a good probe of the transport properties of the medium. Due to the large $c-$quark mass, the charm equilibration time is expected to be much larger (about a factor of 6) than the the light quark equilibration time. Thus it is expected that the elliptic flow of charm quarks will be smaller than the flow of light hadrons. In addition, because charm is produced through hard-scattering, without the collective expansion, the spectral shapes of D-mesons will follow a power-law distribution which deviates strongly from the thermal spectrum. The equilibration time will control the extent to which the

initial power-law spectrum approaches the thermal spectrum. Energy loss in the medium, which is measured through the nuclear modification factor R_{AA} also affects the spectral shapes and the anisotropic flow patterns. Measurements of charm $v2$ and R_{AA} provide a link to the charm the diffusion coefficient, which is a needed input to microscopic transport models addressing thermalization.

Measurements of open charm production and flow in heavy ion collisions are challenging due to the small production cross-sections and the experimental limitations for charm particle identification. The direct reconstruction of $D^0(\overline{D^0}) \rightarrow K^{\mp}\pi^{\pm}$ is subject to large combinatorial background. The STAR collaboration has published D^0 from $d+Au$ collisions [105] and obtained preliminary data from $Au+Au$ collisions [106], however the large multiplicities in heavy ion collisions result in signal-to-background ratios of the order 1/1000 and corresponding systematic errors on the D^0 yields of order 30%. Measurements of charm flow and nuclear modification factors (R_{AA}) with combined statistical and systematic uncertainties $<\sim 10\%$ are needed in order to constrain theoretical models and give insight into charm diffusion coefficients. Charm measurements using non-photonic electrons, which primarily originate from charm semileptonic decays have been performed both in PHENIX [107, 108, 109, 110] and in STAR [106]. The systematic uncertainties in the p_T spectra measured by PHENIX are of order 10% at $p_T = 0.4$ GeV/c and increase to 15% high-p_T ($p_T \simeq 5$ GeV/c). Further improvements in the systematic uncertainties from the single electron charm measurements are difficult to achieve, while reducing the statistical errors is not possible without the RHIC II luminosity upgrade. Recent (preliminary) results for R_{AA} and v_2 of open charm obtained from the PHENIX and STAR electron measurements [111, 112] are shown in Figure 6, Figure 7 and Figure 8. These results utilize the high statistic $Au+Au$ data sample from Run4 of RHIC. Together with improved triggering and reduced background due to material in the PHENIX detector these preliminary results give a factor of 100 statistical improvement over the previously published results. While the $R_{AA}(p_T)$ measurement already has discriminative power, the statistical errors on the v_2 results can not be improved without the RHIC II luminosity upgrade. Another essential experimental improvement will be achieved with the planned vertex detector upgrades in PHENIX and STAR, which will make possible direct charm and beauty identification over a broad kinematic range.

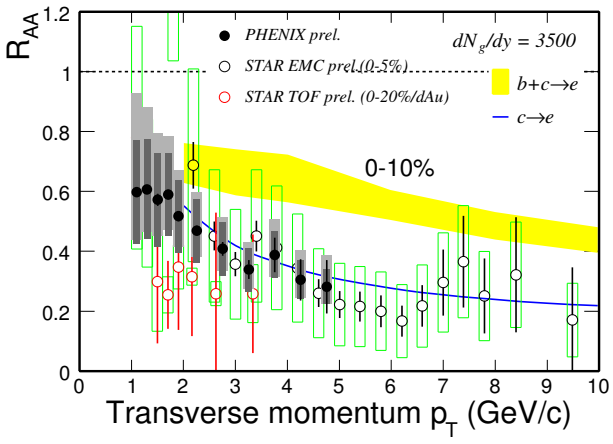

Figure 6: "Non-photonic" electron for 0-10% centrality bin compared with theoretical predictions. from [113].

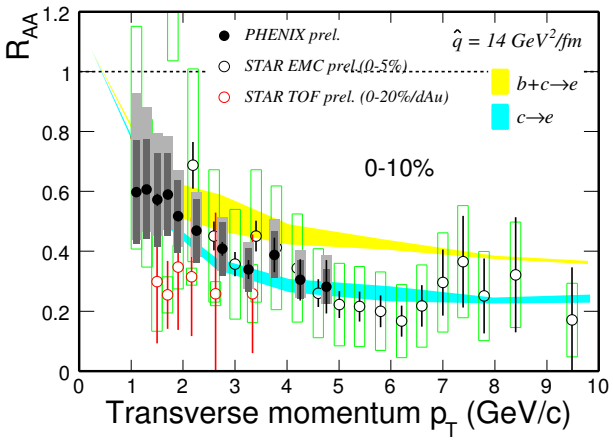

Figure 7: "Non-photonic" electron for 0-10% centrality bin compared with theoretical predictions. from [115].

6 Hadronization

Hadronization is the fundamental process in which the partonic medium converts into hadrons. It includes both the dressing of quarks from their bare masses, thus breaking the approximate chiral symmetry, and the confinement of quarks into colorless hadrons. Due to its non-perturbative nature, the hadronization process is not well understood. Heavy ion reactions present an opportunity to study this process in the nucleus (using $d+A$ collisions) and in the dense QGP medium ($A+A$ collisions). The detailed understanding of hadronization also plays a crucial role for isolating signatures sensitive to the QGP properties and evolution from those which are dominated by the later reaction stages. A conclusive experimental evidence for hadronization occurring from thermalized quark and gluon distributions can be interpreted as an evidence for QGP formation. One of the theoretical milestones of the first several years of the RHIC program was the development of the recombination plus fragmentation model as the standard model of hadronization for matter at intermediate and high transverse momenta: at the center of the recombination + fragmentation model is the realization that hadron production at momenta of a few GeV/c in an environment with a high density of partons occurs by recombination, rather than fragmentation, of partons. It is found that recombination always dominates over fragmentation for an exponentially falling parton spectrum, but that fragmentation wins out eventually, when the spectrum takes the form of a power law.

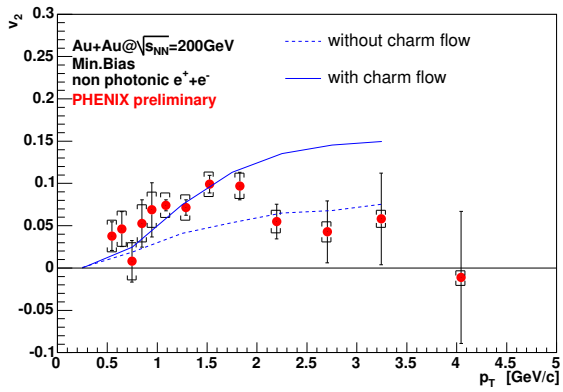

Figure 8: "Non-photonic" electron v_2 compared with theoretical predictions for charm quark flow [116].

In the fragmentation picture [117] the single parton spectrum is convolved with the probability for a parton i to hadronize into a hadron h, which carries a fraction $z < 1$ of the momentum of the parent parton. It has been argued that the fragmentation functions $D_{i\to h}(z)$ can be altered by the environment [118]. The dominant modification mechanism is the energy loss of the propagating parton in the surrounding medium, which leads, in first approximation, to a rescaling of the variable z. This would affect all produced hadrons in the same way, in contradiction with the observations at RHIC.

In the recombination picture, three quarks or a quark/antiquark pair in a densely populated phase space can form a baryon or meson respectively. The amplitude for this process is determined by the hadron wave function. This mechanism has recently been identified as the source of unnatural isospin ratios in the production of D-mesons in the fragmentation region in $\pi^- + A$ interactions at Fermilab [119]. Hadron production in heavy ion collisions by recombination of quarks has been considered before [120], primarily at small transverse momentum.

A major RHIC discovery is the strong nuclear suppression of the pion and inclusive charged hadron yields at transverse momenta larger than 2 GeV/c in central Au + Au collisions, compared to $p+p$ interactions [121]. This is widely seen as the experimental confirmation of jet quenching, the phenomenon that high energy partons lose energy when they travel through the hot medium created in a heavy ion collision [122, 123, 124], entailing a suppression of intermediate and high p_T hadrons.

Another RHIC discovery that prompted the development of the recombination models of hadronization, is that the amount of suppression at intermediate p_T seems to depend on the hadron species. In fact, in the production of protons and anti-protons between 2 and 4 GeV/c the suppression seems to be completely absent. Generally, pions and kaons appear to suffer from a strong energy loss while baryons and anti-baryons do not. Two stunning experimental facts exemplify this [125, 126]. First, the ratio of protons over positively charged pions is equal or above one for $p_T > 1.5$GeV/c and is approximately constant up to 4 GeV/c. Second, the nuclear suppression factor R_{AA} below 4 GeV/c is close to one for protons and lambdas [128], while it is about 0.3 for pions.

The recombination approach [129, 130, 131, 132] has been able to account for the above baryon/meson differences. Additionally, it was observed that the elliptic flow pattern of different hadron species can be explained by a simple recombination mechanism [133, 134, 135, 136]. The anisotropies ,v_2, for the different hadrons are compatible with a universal value of v_2 in the parton phase, related to the hadronic flow by factors of two and three depending on the number of valence quarks [137, 138].

Surprisingly, experimental studies of jet-correlations using identified baryon or meson triggers in the intermediate p_T region show little or no particle species dependence [127], which rules out recombination from a pure thermal source. For the recombination picture to remain valid, at least one of the quarks in the baryon has to come from the fragmentation of a hard-scattered parton and thus preserve the jet-like correlations between the final hadrons.

A detailed study of the interplay of recombination and fragmentation will require high precision data on identified particle distributions covering $p_T \approx< 8$ GeV/c. Of particular interest will be data on multi-strange hadrons and resonances. Resonances have been predicted to violate the elliptic flow scaling law [139], allowing for further insight into the strength of hadronic final state interactions. In addition, the measurement of dynamical two-particle correlations will help to constrain the recombination formalism and the transition to fragmentation at high p_T [140]. Enhanced PID capabilities will become available after the planned STAR and PHENIX upgrades, while the RHIC II luminosity is needed to obtain statistically significant elliptic flow and correlation results involving rare particle species.

There have been attempts to describe the different behavior of baryons and mesons through the existence of gluon junctions [141]. This approach poses the fundamental question about the nature of the baryon number. Detailed baryon number versus charge transport measurements are needed to enable the experimental test of how both the charge and the baryon

number are carried by the quarks. If there is no gluon contribution to the baryon number, then the ratio of charge-to-baryon number in any rapidity or momentum bin should remain fixed to the charge-to-baryon ratio in the initial nuclei. This simple idea is very difficult to test, since a full account for the baryon number transport requires detection of *all* baryons and anti-baryons, not just the charged and/or the weakly decaying neutral baryons. None of the RHIC experiments is equipped with a hadronic calorimeter (except the ZDCs and the PHENIX forward calorimeter FCAL) and thus neutron detection is not possible. The PHENIX experiment has demonstrated that they can identify anti-neutrons using the large annihilation energy deposited in the electromagnetic calorimeter. If one assumes that $\overline{p}/p = \overline{n}/n$, then the gluon junction versus quark baryon stopping could in principle be tested using measured identified charged hadron ratios [142], but in order to have discriminative power the π^-/π^+ ratios need to be measured to a precision better than 0.5%, which is difficult to achieve. Thus, a high-precision baryon versus charge transport measurement needs a careful systematic study of charged particle yields and neutron PID that would require new detectors, not considered in the present upgrades to STAR and PHENIX. A BRAHMS-like spectrometer which includes a hadronic calorimeter in addition to high p_T PID for charged hadrons could enable the measurement of baryon and charge transport over a broad kinematic range. RHIC II luminosity will be required due to the small acceptance of such a device at any particular setting. Another approach to test baryon junction/anti-junction contribution to $B\overline{B}$ production is to study long range rapidity correlations between in baryons and anti-baryons. Identified particle measurements over $|y_B - y_{\overline{B}}| < 2$ as suggested in [143, 144] could be done with the upgraded STAR detector.

All approaches to the study of hadronization ultimately require PID for baryons and mesons over a broad kinematic range with statistically significant samples that will allow for correlation studies including the rare multi-strange baryons and thus critically depend on detector upgrades and increased luminosity.

7 Summary

In summary, the EoS working group has identified the key physics questions related to the bulk properties of the matter created at RHIC that presently remain unanswered: the nature of the transition from hadron gas to QGP and the location of the critical point in the QCD phase diagram, the evolution of the QCD EoS through the transition region, dissipative

effects in the sQGP medium, the thermalization mechanism and relation to sQGP properties, the hadronization mechanism and the nature of the baryon number.

Progress on many fronts requires both theoretical and experimental developments and feedback between the two. Although a lot has been learned from the first few years of RHIC about the collective behavior and thermodynamics properties of hot and dense QCD matter, in many cases our understanding is incomplete. The theoretical models are as yet too idealized or have too many parameters that can not be fixed without precision experimental input. The approaches that will lead to further development can be classified in the following groups:

- Energy scans

  An energy scan between $\sqrt{s_{NN}} = 5 - 62$ GeV will enable the search for the critical point in the QCD phase diagram, which may be observed via fluctuation and correlation measurements. The evolution of the QCD EoS could be studied via the measurements of identified particle single spectra and elliptic flow, correlating thermal photons and particle multiplicity measurements, or using photon HBT correlations.

- Species scans

  Using $U + U$ collisions will allow for the exploration of new regions of energy density versus deformation space and provide constraints to viscosity in the sQGP phase. Asymmetric species scans will allow for further constraints in the hydrodynamics description of heavy ion collisions, including viscosity, by introducing odd-harmonics (i.e. v_3) in the azimuthal distributions of particle emission, which will provide additional sensitivity to the dynamics of the collisions.

- Rare probe measurements

  Statistically significant measurements of spectra, elliptic flow, nuclear modification factors, baryon/meson ratios, identified particle correlations of ϕ, Ξ, Ω, D covering intermediate and high p_T will aid in disentangling viscosity in the partonic and the hadronic medium, reveal thermalization mechanisms, and provide insight in the hadronization process.

All of these measurements require significantly increased luminosity either to provide large statistics, or as in the case of energy scan - several different experimental settings. Forward detector upgrades with PID are crucial for the success of the asymmetric species and $U + U$

program. The charm measurements require μ-vertex detection. The program outlined in this document can be completed at the RHIC II facility.

8 Acknowledgment

We acknowledge the contribution of F.Karsch, W. Fischer, T. Hirano, D. Teaney, U. Heinz, V. Greco, D. d'Enterria, S.Panitkin, R. Witt, A. Kuhlman, P. Stankus, J. Thomas, L. Ruan, G. van Nieuwenhuizen, M. Lamont, A. Milov and E. Kistenev who made presentations at the EoS working group meetings and many others who contributed for lively discussions at the meetings and on the mailing list.

References

[1] T. Satogata, EPAC-2004-TUXLH03 *Presented at the 9th European Particle Accelerator Conference (EPAC 2004), Lucerne, Switzerland, 5-9 Jul 2004*

[2] J. Adams *et al.*[STAR Collaboration], Phys. Lett. **B 616**, 8 (2005)

[3] K. G. Wilson, Phys. Rev. D **10**, 2445 (1974).

[4] M. Creutz, L. Jacobs and C. Rebbi, Phys. Rept. **95**, 201 (1983).

[5] F. Karsch, E. Laermann and A. Peikert, Phys. Lett. B **478**, 447 (2000) [arXiv:hep-lat/0002003].

[6] Y. Aoki, Z. Fodor, S. D. Katz and K. K. Szabo, arXiv:hep-lat/0510084.

[7] I. Arsene *et al.* [BRAHMS Collaboration], Nucl. Phys. A **757**, 1 (2005) [arXiv:nucl-ex/0410020]. K. Adcox *et al.* [PHENIX Collaboration], Nucl. Phys. A **757**, 184 (2005) [arXiv:nucl-ex/0410003]. B. B. Back *et al.*, Nucl. Phys. A **757**, 28 (2005) [arXiv:nucl-ex/0410022]. J. Adams *et al.* [STAR Collaboration], Nucl. Phys. A **757**, 102 (2005) [arXiv:nucl-ex/0501009].

[8] F. Karsch, J. Phys. G **31**, S633 (2005) [arXiv:hep-lat/0412038].

[9] C. Bernard *et al.* [MILC Collaboration], Phys. Rev. D **71**, 034504 (2005) [arXiv:hep-lat/0405029].

[10] M. G. Alford, K. Rajagopal and F. Wilczek, Phys. Lett. B **422**, 247 (1998) [arXiv:hep-ph/9711395].

[11] R. Rapp, T. Schafer, E. V. Shuryak and M. Velkovsky, Phys. Rev. Lett. **81**, 53 (1998) [arXiv:hep-ph/9711396].

[12] M. A. Stephanov, K. Rajagopal and E. V. Shuryak, Phys. Rev. Lett. **81**, 4816 (1998) [arXiv:hep-ph/9806219].

[13] Z. Fodor and S. D. Katz, JHEP **0203**, 014 (2002) [arXiv:hep-lat/0106002].

[14] R. Gavai, S. Gupta and R. Ray, Prog. Theor. Phys. Suppl. **153**, 270 (2004) [arXiv:nucl-th/0312010].

[15] C. R. Allton *et al.*, Phys. Rev. D **66**, 074507 (2002) [arXiv:hep-lat/0204010].

[16] M. D'Elia and M. P. Lombardo, Phys. Rev. D **67**, 014505 (2003) [arXiv:hep-lat/0209146].

[17] Z. Fodor, S. D. Katz and K. K. Szabo, Phys. Lett. B **568**, 73 (2003) [arXiv:hep-lat/0208078].

[18] C. R. Allton, S. Ejiri, S. J. Hands, O. Kaczmarek, F. Karsch, E. Laermann and C. Schmidt, Phys. Rev. D **68**, 014507 (2003) [arXiv:hep-lat/0305007].

[19] R. V. Gavai and S. Gupta, Phys. Rev. D **71**, 114014 (2005) [arXiv:hep-lat/0412035].

[20] Z. Fodor and S. D. Katz, JHEP **0404**, 050 (2004) [arXiv:hep-lat/0402006].

[21] S. Ejiri, C. R. Allton, S. J. Hands, O. Kaczmarek, F. Karsch, E. Laermann and C. Schmidt, Prog. Theor. Phys. Suppl. **153**, 118 (2004) [arXiv:hep-lat/0312006].

[22] C. R. Allton, S. Ejiri, S. J. Hands, O. Kaczmarek, F. Karsch, E. Laermann and C. Schmidt, Nucl. Phys. Proc. Suppl. **141**, 186 (2005) [arXiv:hep-lat/0504011].

[23] K. Rajagopal, Acta Phys. Polon. B **31**, 3021 (2000) [Comments Nucl. Part. Phys. A **2**, 120 (2002 APCPC,549,95-119.2002)] [arXiv:hep-ph/0009058].

[24] T. Anticic *et al.* [NA49 Collaboration], Phys. Rev. C **70**, 034902 (2004) [arXiv:hep-ex/0311009].

[25] H. Appelshauser *et al.* [NA49 Collaboration], Phys. Lett. B **459**, 679 (1999) [arXiv:hep-ex/9904014].

[26] K. Adcox *et al.* [PHENIX Collaboration], Phys. Rev. C **66**, 024901 (2002) [arXiv:nucl-ex/0203015].

[27] J. Adams *et al.* [STAR Collaboration], Phys. Rev. C **71**, 064906 (2005) [arXiv:nucl-ex/0308033].

[28] CERES collaboration, D. Adamova *et al.*, Nucl. Phys. **A727**, 97 (2003).

[29] M. M. Aggarwal *et al.* [WA98 Collaboration], Phys. Rev. C **65**, 054912 (2002) [arXiv:nucl-ex/0108029].

[30] C. Alt *et al.* [NA49 Collaboration], Phys. Rev. C **70**, 064903 (2004) [arXiv:nucl-ex/0406013].

[31] K. Adcox *et al.* [PHENIX Collaboration], Phys. Rev. Lett. **89**, 082301 (2002) [arXiv:nucl-ex/0203014].

[32] J. Adams *et al.* [STAR Collaboration], Phys. Rev. C **68**, 044905 (2003) [arXiv:nucl-ex/0307007].

[33] J. Adams *et al.* [STAR Collaboration], arXiv:nucl-ex/0509030.

[34] A. Andronic, P. Braun-Munzinger and J. Stachel, arXiv:nucl-th/0511071.

[35] P. Braun-Munzinger *et al.* Nucl. Phys. **A681** 119 (2001)

[36] T. Satogata, URL:www.bnl.gov/rhic_ags/users_meeting/Agenda/Fri.asp *A talk presented at the RHIC-AGS Users' Meeting, 9 Jun, 2006*

[37] P. Staszel [BRAHMS Collaboration], arXiv:nucl-ex/0510061.

[38] J. D. Bjorken, Phys. Rev. D **27**, 140 (1983).

[39] R. B. Clare and D. Strottman, Phys. Rept. **141**, 177 (1986).

[40] A. Dumitru and D. H. Rischke, Phys. Rev. C **59**, 354 (1999) [arXiv:nucl-th/9806003].

[41] P. F. Kolb and U. W. Heinz, arXiv:nucl-th/0305084.

[42] P. Huovinen, arXiv:nucl-th/0305064.

[43] T. Hirano and K. Tsuda, Nucl. Phys. A **715**, 821 (2003) [arXiv:nucl-th/0208068].

[44] D. Teaney, J. Lauret and E. V. Shuryak, arXiv:nucl-th/0110037.

[45] U. W. Heinz and P. F. Kolb, arXiv:hep-ph/0204061.

[46] D. Teaney, Nucl. Phys. A **715**, 817 (2003) [arXiv:nucl-th/0209024].

[47] D. Zschiesche, S. Schramm, H. Stoecker and W. Greiner, Phys. Rev. C **65**, 064902 (2002) [arXiv:nucl-th/0107037].

[48] T. Renk, arXiv:hep-ph/0408218.

[49] P. Huovinen, Nucl. Phys. A **761**, 296 (2005) [arXiv:nucl-th/0505036].

[50] B. Kampfer, M. Bluhm, R. Schulze, D. Seipt and U. Heinz, arXiv:hep-ph/0509146.

[51] Y. Hama, R. P. G. Andrade, F. Grassi, O. J. Socolowski, T. Kodama, B. Tavares and S. S. Padula, "3D relativistic hydrodynamic computations using lattice-QCD inspired equations of state," arXiv:hep-ph/0510096.

[52] B. B. Back *et al.* [PHOBOS Collaboration], Phys. Rev. C **72**, 051901 (2005) [arXiv:nucl-ex/0407012].

[53] U. W. Heinz and A. Kuhlman, Phys. Rev. Lett. **94**, 132301 (2005) [arXiv:nucl-th/0411054].

[54] A. J. Kuhlman and U. W. Heinz, Phys. Rev. C **72**, 037901 (2005) [arXiv:nucl-th/0506088].

[55] Documentation on the EBIS facility can be found at this URL: www.c-ad.bnl.gov/ebis

[56] C. Adler *et al.* [STAR Collaboration], Phys. Rev. C **66**, 034904 (2002).

[57] C. Alt *et al.* [NA49 Collaboration], Phys. Rev. C **68**, 034903 (2003).

[58] B. B. Back *et al.* [PHOBOS Collaboration], Phys. Rev. Lett. **89**, 222301 (2002).

[59] T. Hirano, Phys. Rev. C **65**, 011901(R) (2002).

[60] U. Heinz and P. F. Kolb, J. Phys. G **30**, S1229 (2004).

[61] P. F. Kolb, J. Sollfrank, and U. Heinz, Phys. Rev. C **62**, 054909 (2000).

[62] Other more technical roots of this tendency were suggested by M. Miller and R. Snellings, nucl-ex/0312008.

[63] U. Heinz and P. F. Kolb, Nucl. Phys. A **702**, 269 (2002).

[64] J. Y. Ollitrault, Phys. Rev. D **46**, 229 (1992).

[65] J. F. Owens, Rev. Mod. Phys. **59**, 465 (1987).

[66] A. Dumitru, D. H. Rischke, H. Stöcker and W. Greiner. Mod. Phys. Lett. **A8** (1993) 1291.

[67] J. Alam, D. K. Srivastava, B. Sinha and D. N. Basu. Phys. Rev. **D48** (1993) 1117.

[68] C. T. Traxler, H. Vija, M. H. Thoma. Phys. Lett. **B346** (1995) 329.

[69] A Dumitru, U. Katscher, J. A. Maruhn, H. Stöcker, W. Greiner and D. H. Rischke. Phys. Rev. **C51** (1995) 2166.

[70] J. J. Neumann, D. Seibert and G. Fai. Phys. Rev. **C51** (1995) 1460.

[71] D. d'Enterria and D. Peressounko, arXiv:nucl-th/0503054.

[72] D. K. Srivastava and J. I. Kapusta, Phys. Lett. B **307**, 1 (1993); D. K. Srivastava and J. I. Kapusta, Phys. Rev. C **48**, 1335 (1993); D. K. Srivastava, Phys. Rev. D **49**, 4523 (1994); D. K. Srivastava and C. Gale, Phys. Lett. B **319**, 407 (1994); D. K. Srivastava and J. I. Kapusta, Phys. Rev. C **50**, 505 (1994).

[73] A. Timmermann, M. Plümer, L. Razumov, and R. M. Weiner, Phys. Rev. C **50**, 3060 (1994).

[74] J. Pisut, N. Pisutova and B. Tomasik, Phys. Lett. B **345**, 553 (1995), [Erratum-ibid. B **353**, 606 (1995)].

[75] C. Slotta and U. W. Heinz, Phys. Lett. B **391**, 469 (1997).

[76] D. Peressounko, Phys. Rev. C **67**, 014905 (2003).

[77] J. Alam, B. Mohanty, P. Roy, S. Sarkar, and B. Sinha, Phys. Rev. C **67**, 054902 (2003).

[78] D. K. Srivastava, Phys. Rev. C **71**, 034905 (2005) [arXiv:nucl-th/0411041].

[79] B. Muller and K. Rajagopal, Eur. Phys. J. C **43**, 15 (2005).

[80] S. Pal and S. Pratt, Phys. Lett. B **578**, 310 (2004).U=U

[81] D. Teaney, arXiv:nucl-th/0301099.

[82] G. Policastro, D. T. Son and A. O. Starinets, Phys. Rev. Lett. **87**, 081601 (2001) [arXiv:hep-th/0104066].

[83] A. Nakamura and S. Sakai, Phys. Rev. Lett. **94**, 072305 (2005) [arXiv:hep-lat/0406009].

[84] T. Hirano and M. Gyulassy, arXiv:nucl-th/0506049.

[85] S. A. Bass and A. Dumitru, Phys. Rev. C **61**, 064909 (2000) [arXiv:nucl-th/0001033].

[86] D. Teaney, J. Lauret and E. V. Shuryak, Phys. Rev. Lett. **86**, 4783 (2001) [arXiv:nucl-th/0011058].

[87] T. Hirano, arXiv:nucl-th/0510005.

[88] C. Nonaka and S. A. Bass, arXiv:nucl-th/0510038.

[89] M. Oldenburg [STAR Collaboration], arXiv:nucl-ex/0510026.

[90] D. Pal [PHENIX Collaboration], arXiv:hep-ex/0510020.

[91] X. Dong, S. Esumi, P. Sorensen, N. Xu and Z. Xu, Phys. Lett. **B 597** (2004) 328.

[92] S. Gupta, Phys. Lett. B **597**, 57 (2004) [arXiv:hep-lat/0301006].

[93] G. D. Moore and D. Teaney, Phys. Rev. C **71**, 064904 (2005) [arXiv:hep-ph/0412346].

[94] H. van Hees, V. Greco and R. Rapp, arXiv:nucl-th/0508055.

[95] P. B. Gossiaux, V. Guiho and J. Aichelin, J. Phys. G **31**, S1079 (2005) [arXiv:hep-ph/0411324].

[96] J. Ruppert and B. Muller, Phys. Lett. B **618**, 123 (2005) [arXiv:hep-ph/0503158].

[97] J. Casalderrey-Solana, E. V. Shuryak and D. Teaney, arXiv:hep-ph/0411315.

[98] H. Stoecker, Nucl. Phys. A **750**, 121 (2005) [arXiv:nucl-th/0406018].

[99] T. Renk and J. Ruppert, arXiv:hep-ph/0509036.

[100] V. Koch, A. Majumder and X. N. Wang, arXiv:nucl-th/0507063.

[101] S. S. Adler *et al.* (PHENIX Collaboration), [arXiv:nucl-ex/0507004]

[102] J . Adams *et al.* (STAR Collaboration), *Phys. Rev. Lett.* **95** (2005) 152301

[103] J. Casalderrey-Solana, E. V. Shuryak, D. Teaney, arXiv:hep-ph/0610283

[104] A. K. Chaudhuri and U. Heinz, [arXiv:nucl-th/0503028]

[105] J. Adams *et al.* [STAR Collaboration], Phys. Rev. Lett. **94**, 062301 (2005) [arXiv:nucl-ex/0407006].

[106] H. Zhang, arXiv:nucl-ex/0510063.

[107] S. S. Adler *et al.* [PHENIX Collaboration], arXiv:nucl-ex/0510047.

[108] S. S. Adler *et al.* [PHENIX Collaboration], Phys. Rev. C **72**, 024901 (2005) [arXiv:nucl-ex/0502009].

[109] S. S. Adler *et al.* [PHENIX Collaboration], Phys. Rev. Lett. **94**, 082301 (2005) [arXiv:nucl-ex/0409028].

[110] K. Adcox *et al.* [PHENIX Collaboration], Phys. Rev. Lett. **88**, 192303 (2002) [arXiv:nucl-ex/0202002].

[111] S. A. Butsyk *et al.* [PHENIX Collaboration] arXiv:nucl-ex/0510010 (2005).

[112] X. Dong *et al.* [STAR Collaboration] arXiv:nucl-ex/0509038 (2005).

[113] M. Djordjevic, M. Gyulassy, S. Wicks, Phys. Rev. Lett. **94**, 112301 (2005).

[114] N. Armesto, S. Dainese, C. Salgado, and U. Wiedemann, Phys. Rev. **D71**, 054027 (2005).

[115] N. Armesto et al., arXiv:hep-ph/0510284 and arXiv:hep-ph/0511257 (2005).

[116] V. Greco, C. M. Ko, R. Rapp, Phys. Lett. **B595**, 202 (2004).

[117] J. C. Collins and D. E. Soper, Nucl. Phys. B **194**, 445 (1982).

[118] X. F. Guo and X. N. Wang, Phys. Rev. Lett. **85**, 3591 (2000); Nucl. Phys. A **696**, 788 (2001).

[119] E. Braaten, Y. Jia and T. Mehen, Phys. Rev. Lett. **89**, 122002 (2002).

[120] C. Gupt, R. K. Shivpuri, N. S. Verma and A. P. Sharma, Nuovo Cim. A **75**, 408 (1983); T. S. Biro, P. Levai and J. Zimanyi, Phys. Lett. B **347**, 6 (1995); T. S. Biro, P. Levai and J. Zimanyi, J. Phys. G **28**, 1561 (2002).

[121] K. Adcox *et al.* [PHENIX Collaboration], Phys. Rev. Lett. **88**, 022301 (2002); C. Adler *et al.* [STAR Collaboration], Phys. Rev. Lett. **90**, 082302 (2003). I. Arsene *et al.* [BRAHMS Collaboration], Phys. Rev. Lett. **91**, 072305 (2003); B.B. Back *et al.* [PHOB0S Collaboration], Phys. Lett. **B578**, 297 (2004);

[122] J. D. Bjorken, FERMILAB-PUB-82-059-THY (1982); M. H. Thoma and M. Gyulassy, Nucl. Phys. B **351**, 491 (1991); X. N. Wang and M. Gyulassy, Phys. Rev. Lett. **68**, 1480 (1992); M. Gyulassy and X. Wang, Nucl. Phys. B **420**, 583 (1994); R. Baier, Y. L. Dokshitzer, A. H. Mueller, S. Peigne and D. Schiff, Nucl. Phys. B **483**, 291 (1997); B. G. Zakharov, JETP Lett. **65**, 615 (1997) M. Gyulassy, P. Levai and I. Vitev, Phys. Rev. Lett. **85**, 5535 (2000) U. A. Wiedemann, Nucl. Phys. B **588**, 303 (2000)

[123] R. Baier, Y. L. Dokshitzer, A. H. Mueller and D. Schiff, JHEP **0109**, 033 (2001);

[124] B. Müller, Phys. Rev. C *in print* (2003), nucl-th/0208038.

[125] K. Adcox *et al.* [PHENIX Collaboration], Phys. Rev. Lett. **88**, 242301 (2002) [arXiv:nucl-ex/0112006].

[126] S. S. Adler *et al.* [PHENIX Collaboration], Phys. Rev. Lett. **91**, 172301 (2003) [arXiv:nucl-ex/0305036].

[127] S. S. Adler *et al.* [PHENIX Collaboration], Phys. Rev. C **71**, 051902 (2005) [arXiv:nucl-ex/0408007].

[128] J. Adams *et al.* [STAR Collaboration], Phys. Rev. Lett. **92**, 052302 (2004) [arXiv:nucl-ex/0306007].

[129] R. J. Fries, B. Müller, C. Nonaka and S. A. Bass, Phys. Rev. Lett. **90**, 202303 (2003).

[130] R. J. Fries, B. Muller, C. Nonaka and S. A. Bass, Phys. Rev. C **68**, 044902 (2003) [arXiv:nucl-th/0306027].

[131] V. Greco, C. M. Ko and P. Levai, Phys. Rev. Lett. **90**, 202302 (2003).

[132] R. C. Hwa and C. B. Yang, nucl-th/0211010.

[133] Z. W. Lin and C. M. Ko, Phys. Rev. Lett. **89**, 202302 (2002).

[134] S. A. Voloshin, Nucl. Phys. A **715**, 379c (2003).

[135] D. Molnár and S. A. Voloshin, Phys. Rev. Lett. **91**, 092301 (2003) [arXiv:nucl-th/0302014].

[136] Z. Lin and D. Molnár, Phys. Rev. C **68**, 044901 (2003) [arXiv:nucl-th/0304045].

[137] P. Sorensen for the STAR Collaboration, J. Phys. G **30**, S217 (2004) [arXiv:nucl-ex/0305008].

[138] S. S. Adler *et al.* [PHENIX Collaboration], Phys. Rev. Lett. **91**, 182301 (2003) [arXiv:nucl-ex/0305013].

[139] C. Nonaka, B. Muller, M. Asakawa, S. A. Bass and R. J. Fries, Phys. Rev. C **69**, 031902 (2004) [arXiv:nucl-th/0312081].

[140] R. J. Fries, S. A. Bass and B. Muller, Phys. Rev. Lett. **94**, 122301 (2005) [arXiv:nucl-th/0407102].

[141] I. Vitev and M. Gyulassy, Phys. Rev. C **65**, 041902 (2002).

[142] P. Stankus. A talk given at the PANIC 05 conference, Santa Fe, NM, Oct 24-28, 2005

[143] V. Topor Pop, M. Gyulassy, J. Barrette, and C. Gale, X. N. Wang and N. Xu, Phys. Rev. C **70**, 064906 (2004).

[144] V. Topor Pop, M. Gyulassy, J. Barrette, and C. Gale, Phys. Rev. C **72**, 054901 (2005).